

Mach stem formation in explosion systems, which include high modulus elastic elements

Igor A. Balagansky, Kazuyuki Hokamoto, Palavesamuthu Manikandan, Alexander D. Matrosov, Ivan A. Stadnichenko, Hitoshi Miyoshi, Ivan A. Bataev, and Anatoly A. Bataev

Citation: *Journal of Applied Physics* **110**, 123516 (2011); doi: 10.1063/1.3671063

View online: <http://dx.doi.org/10.1063/1.3671063>

View Table of Contents: <http://scitation.aip.org/content/aip/journal/jap/110/12?ver=pdfcov>

Published by the [AIP Publishing](#)

Articles you may be interested in

[Generation of fast cumulative water jets by underwater electrical explosion of conical wire arrays](#)
J. Appl. Phys. **117**, 015901 (2015); 10.1063/1.4905548

[Indirect detonation initiation using acoustic timescale thermal power deposition](#)
Phys. Fluids **25**, 091113 (2013); 10.1063/1.4820130

[Proton Radiography Experiments on Shocked High Explosive Products](#)
AIP Conf. Proc. **706**, 839 (2004); 10.1063/1.1780367

[Explosive response model evaluation using the explosive H6](#)
AIP Conf. Proc. **505**, 805 (2000); 10.1063/1.1303593

[Single and multiple impact ignition of new and aged high explosives in the Steven Impact Test](#)
AIP Conf. Proc. **505**, 663 (2000); 10.1063/1.1303560



SHIMADZU Powerful, Multi-functional UV-Vis-NIR and FTIR Spectrophotometers

Excellence in Science

Providing the utmost in sensitivity, accuracy and resolution for applications in materials characterization and nano research

- Photovoltaics
- Polymers
- Thin films
- Paints
- Ceramics
- DNA film structures
- Coatings
- Packaging materials

[Click here to learn more](#)



Mach stem formation in explosion systems, which include high modulus elastic elements

Igor A. Balagansky,^{1,a)} Kazuyuki Hokamoto,² Palavesamuthu Manikandan,² Alexander D. Matrosov,³ Ivan A. Stadnichenko,³ Hitoshi Miyoshi,⁴ Ivan A. Bataev,¹ and Anatoly A. Bataev¹

¹*Novosibirsk State Technical University, Novosibirsk 630092, Russia*

²*Shock Wave and Condensed Matter Research Center, Kumamoto University, Kumamoto 860-8555, Japan*

³*Lavrentyev Institute of Hydrodynamics SB RAS, Novosibirsk 630090, Russia*

⁴*Chugoku Kayaku Co., Ltd., Chugoku, Tokyo 103-0023, Japan*

(Received 30 August 2011; accepted 15 November 2011; published online 23 December 2011)

Results of experimental and numerical research of the Mach stem formation in explosion systems, which include high modulus elastic elements, are presented. The experimental data are discussed, and the analysis using ANSYS AUTODYN 11.0 is provided. It is shown that the phenomenon is reproduced for various high explosives. The Mach stem formation is observed in the conditions close to critical conditions of detonation transfer from an active to a passive HE charge. The best conditions for the Mach stem formation have been observed for TG-40/60 (Russian analog of Composition B) with silicon carbide insert heights of 16.5 mm, 18 mm, and 19.5 mm. The physical reason of the phenomenon is the propagation of a convergent detonation wave into highly compressed HE. The phenomenon is reproduced in numerical simulation with ANSYS AUTODYN 11.0. Calculated maximum value of pressure on the symmetry axis of passive HE charge was up to 1.25 Mbar. Results of metallographic analysis of steel identification specimen on the rear end of the passive HE charge indirectly confirm very high local pressures and temperatures for this scheme of explosion loading. © 2011 American Institute of Physics. [doi:10.1063/1.3671063]

I. INTRODUCTION

If we provide a high explosive (HE) charge contact with an inert element having wave velocity greater than detonation velocity, the advanced wave in this element is able to influence layers of undetonated HE and in some cases to lead to interesting effects. The first publication on this topic was devoted to experimental substantiation of practicability of a self-accelerated detonation in HE charge with the axial channel filled with lithium.¹ The phenomenon of the chemical reaction initiation ahead of a detonation wave under the influence of an advanced elastic wave in a cylindrical glass or quartz shell is described in another paper.²

A change of the detonation front shape near the HE/solid material interface and an increase of local detonation velocity near the interface are noted in other papers.^{3,4}

It has been shown that if sound velocity in an inert wall exceeds detonation velocity in HE, a compression wave without shock front extends into the inert wall.^{5,6}

The effect of increased local explosion action was observed in HE charges placed in silicon carbide shells.⁷ For nitromethane, the increase of detonation pressure was up to 56% compared with stationary detonation.

The phenomenon of energy focusing in explosion systems that include high modulus elastic elements was observed in a passive HE charge of cast TG-40/60 without a cumulative shape under shock wave loading by explosion of an active HE charge in water after preliminary compression by a leading wave in a silicon carbide insert.^{8,9} The phenomenon

manifested itself as a hole in the identification steel specimen with depth of about 10 mm and diameter of about 5 mm.

The results of experimental studies of physical reasons and conditions for this phenomenon are presented in another paper.¹⁰ Experiments were conducted to study the conditions of this phenomenon for TG-40/60, SEP and Composition B. The phenomenon was observed in conditions close to critical conditions of detonation transfer from an active to a passive HE charge. The best conditions for the phenomenon were observed for TG-40/60 with ceramic insert heights of 16.5 mm, 18 mm, and 19.5 mm. The physical reason for this focusing process is the propagation of a convergent detonation wave into highly compressed HE and the formation of a Mach stem on the axis of HE charge.

In this paper, the experimental data are discussed in detail, and the analysis using ANSYS AUTODYN 11.0 is provided.

II. EXPERIMENTAL DATA

The scheme of the experimental assembly is shown in Fig. 1. Active and passive HE charges were shaped as cylindrical cartridges with diameter and height of 40 mm. On the rear end of the passive HE charge, an identification steel specimen was mounted to detect the presence or absence of detonation. Inert inserts of silicon carbide were shaped as 20 mm × 20 mm square prisms of varying heights Δ , and were located between active and passive HE charges without any clearance on the way of initiating shock wave and with partial overlap of HE cross sections. Inert inserts were mounted using vacuum lubricant «Ramzai» to prevent any clearance between HE charges and prisms. The experimental

^{a)}Electronic mail: balagansky@craft.nstu.ru.

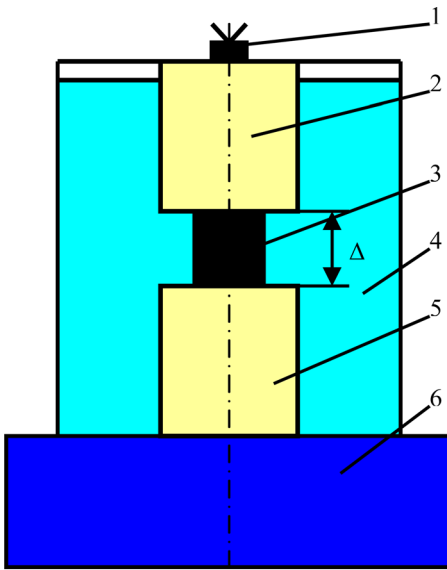


FIG. 1. (Color online) Experimental assembly scheme: 1 - electric detonator; 2 - active HE charge; 3 - inert insert (shaped as a 20 mm × 20 mm square prism); 4 - degassed water; 5 - passive HE charge; 6 - identification steel specimen.

assembly was fastened with three textolite strips (1 mm thick and 10 mm wide) and fixed with Scotch tape. We provided a complete absence of air bubbles in the water.

The density and porosity of silicon carbide were 3.08 g/cm³ and 2%, respectively. After explosion, the surface of the identification specimen in the contact zone beneath the passive HE charge had typical temper colors that demonstrated presence of high temperatures locally. A typical surface of the identification specimen for cast TG-40/60 is shown in Fig. 2. Results of experiments for different HEs and heights of silicon carbide inserts are given in Table I.

Before explosion, the identification specimen had a ferrite-pearlite structure with the average ferrite grain size of 28 μm. We have found that after explosion, the formation of deformation twins is typical not only for ferrite grains, but also for pearlite colonies (see Fig. 3 and Fig. 4).

This behavior is absolutely atypical for usual methods of explosion loading. The second structure peculiarity is the presence of ferrite grains with size of 3–5 μm, which is fairly



FIG. 2. (Color online) A typical surface of a steel identification specimen with a hole caused by the effect of detonation products of a passive HE charge.

TABLE I. Focusing phenomenon presence. [Reprinted with permission from Shock Compression of Condensed Matter. Copyright 2009, American Institute of Physics.]

HE, Density	Height of insert Δ, mm	Number of shots	Result (yes/no)
Cast TG- 40/60, 1.65 g/cm ³ (Russian analog of Composition B)	16.5	1	yes
	18.0	1	yes
	19.5	3	yes
	20.0	2	yes
	24.8	1	no
	18.0	1	yes
Cast Composition B, 1.66–1.67 g/cm ³	20.0	1	no
	10.0	1	no
	15.0	1	yes
	20.0	1	yes

small in comparison with the original structure. That indirectly confirms very high pressures and temperatures for this scheme of explosion loading.

Russian high speed camera VFU was used to record the process in experimental assembly with TG-40/60 and Δ = 19.6 mm. Identification steel specimen was absent in this case. Results are shown in Fig. 5.

The angular velocity of VFU mirror was 53,000 rpm, time separation between pictures was 4.53 μs. Grid cell size was 15 × 15 mm. One can see the following peculiarities of the process: first, the transit time of the shock wave in the passive HE charge was 4.53 μs, which corresponds to the detonation velocity value of 8.9 km/s. Second, when the detonation wave passes through the passive HE charge into water, one can see local heterogeneities on the end face of the charge. We presume that those heterogeneities are related to Taylor instability on the boundary HE/water or to the instability of the detonation front in HE. Third, the shape of the shock wave in water shows that its velocity on symmetry axis is greater than on the periphery.

Recordings with the high speed video camera SHIMADZU HPV-1 were conducted for ceramic insert heights of 15, 16, 17, 18, 20 mm and cast Composition B with density of 1.66–1.67 g/cm³. For those experiments, videos and

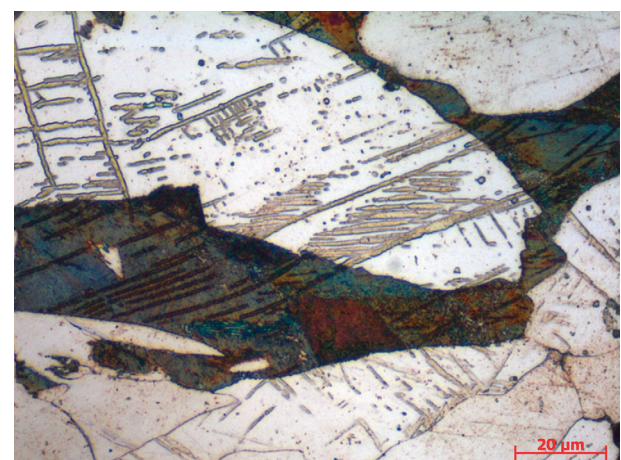


FIG. 3. (Color online) Deformation twins formed in laminated pearlite colonies of the identification specimen (optical microscope).

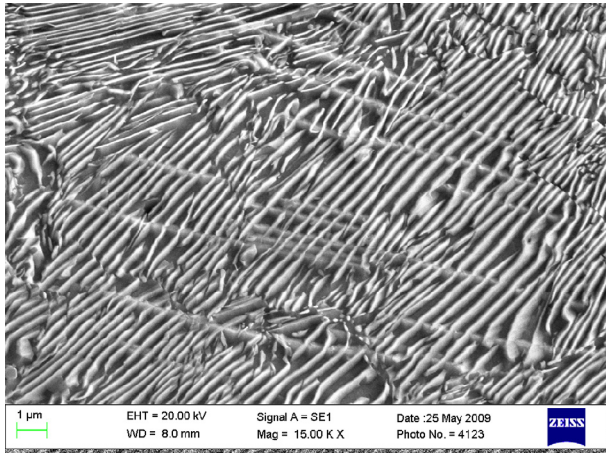


FIG. 4. (Color online) Deformation twins formed in laminated pearlite colonies of the identification specimen (scanning electron microscope).

still frames with time step of $1 \mu\text{s}$ were recorded. A high speed recording was made for experimental assemblies without identification specimen under back-surface impulse lighting (see Fig. 6). In Fig. 6, we can see the plane wave generator, active and passive HE charges, 20 mm ceramic insert, and strips fastened together with Scotch tape.

Photos of 20 mm ceramic inserts with time step of $1 \mu\text{s}$ are shown in Fig. 7. Recorded images for the 20 mm ceramic insert differ essentially from the results for heights of 15, 16, 17, 18 mm, which were similar to each other. We can see that the luminescence of the detonation front is visible inside the HE charge because the shock wave front in water in some cases considerably lags behind the luminous front in the HE charge. The convergent shape of the detonation front in the passive HE charge for the 20 mm insert is worth attention (see Fig. 7, starting with photo #00000031). The three-dimensional effects observed are related to the fact that the ceramic inserts have a square cross-section.

In our opinion, the physical reason of the focusing process lies in the fact that the advanced compression wave in the silicon carbide insert with pressure of 7.5 GPa and front fuzziness of about 3 mm¹¹ enters the passive HE charge from the end face of a ceramic insert, which does not initiate the charge because of its desensitization, but the wave compresses the HE to the pressure of about 2 GPa. Then the shock wave propagates through water to the peripheral area of the passive charge. As a result, the initiation of the passive HE charge occurs on the peripheral area and the detonation wave with a toroid-shaped front moves to the axis of the charge into the high explosive. This leads to a sharp increase of velocity and pressure in the converging detonation wave and to formation of a Mach stem on the axis of the charge.^{12,13} As opposed to other papers, however, this Mach stem propagates in highly compressed HE. Thus, the primary conditions for

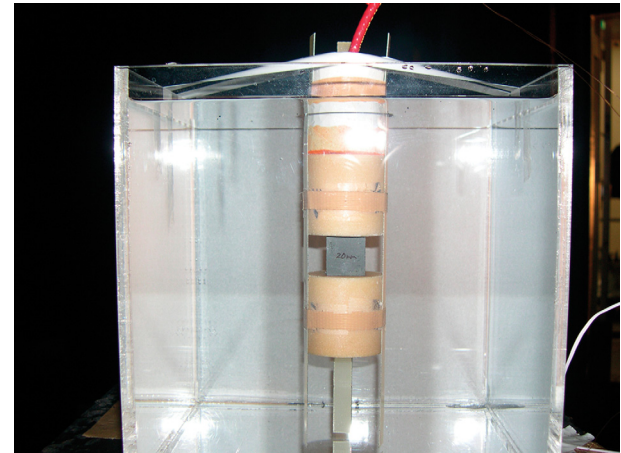


FIG. 6. (Color online) Experimental assembly with a 20 mm ceramic insert. [Reprinted with permission from Shock Compression of Condensed Matter. Copyright 2009, American Institute of Physics.]

the focusing process are the presence of a compressed but undetonated passive HE charge and the converging detonation wave with the collision angle of about 60° ¹³ for Mach stem formation on the axis of the passive HE charge.

III. NUMERICAL SIMULATION

For better understanding of the Mach stem formation phenomenon, we have used numerical simulation with help of ANSYS AUTODYN 11.0.¹⁴ Initial posting corresponded to the experimental assembly for $\Delta = 20 \text{ mm}$ (see Fig. 1). It is shown in Fig. 8.

The simulation was performed in 2D-axis symmetry posting on an Eulerian mesh of 2600×800 cells. After a careful analysis of previously performed simulations on a mesh of 1300×400 cells,¹⁵ we have decided to increase the spatial resolution.

The detonation wave was initiated as a plane wave and propagated from the left to the right boundary of the Eulerian mesh. Boundary conditions on the left, right, and upper boundaries were defined in terms of AUTODYN as “Flow out.” We used values of constants for air, steel, and water from the AUTODYN EOS library.

Behavior of a Composition B passive HE charge with density of 1.63 g/cm^3 was calculated from JWL EOS¹⁶ and Lee-Tarver kinetic constants.¹⁷ We have tested this behavior during computer modeling of the experiments on desensitization of heterogeneous high explosives.^{8,9} Comparison of experimental and numerical results is given in Table II.

Values of the EOS and kinetic constants are given in Table III.

The possibility of using Lee-Tarver kinetic equation to simulate the Mach stem formation follows from the results of previous research.¹⁸

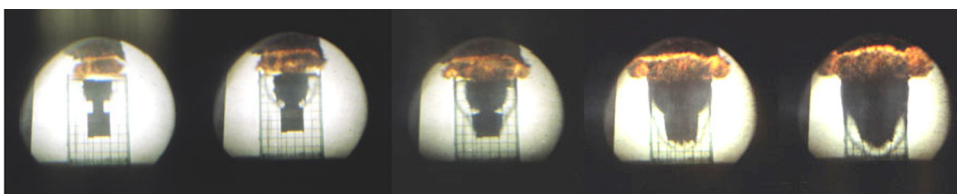


FIG. 5. (Color online) VFU rotating mirror camera records with time step of $4.53 \mu\text{s}$.

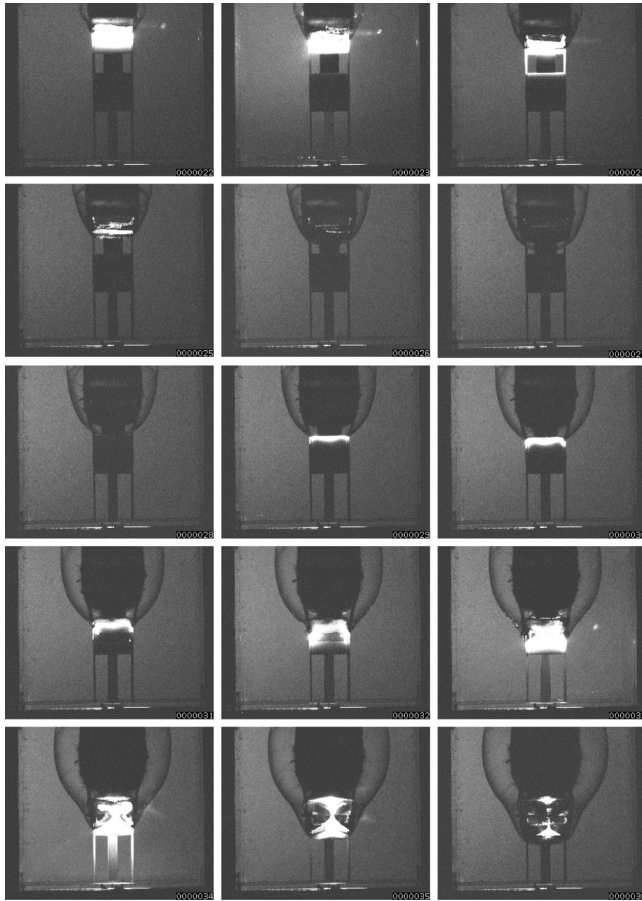


FIG. 7. Optical records for the experimental assembly with a 20 mm ceramic insert. Time step is equal to $1 \mu\text{s}$.

Parameters of EOS for silicon carbide were chosen to reproduce the experimental results on evolution of shock waves in silicon carbide rods.¹¹ Values of the parameters are shown in Table IV.

The results of simulation at different times with initial time of $5 \mu\text{s}$, and time step of $1 \mu\text{s}$ are shown as material flow fields and pressure contours in Fig. 9.

A complex interaction process of shock, detonation and compression waves develops in the assembly. We can see the Mach stem formation in passive HE charge.

The detonation wave profile with C-J pressure of 22.4 GPa in the active HE charge can be seen in Fig. 10.

Figure 11 demonstrates the graph of the axial stress in the silicon carbide insert versus axial distance at the time of $6.75 \mu\text{s}$.

Figure 12 demonstrates the pressure value in the Mach stem at $t = 15.75 \mu\text{s}$. The value is equal to 1.25 Mbar .

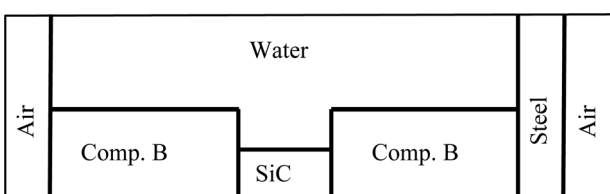


FIG. 8. Initial posting with dimensions of $13.0 \text{ cm} \times 4.0 \text{ cm}$. The bottom boundary is the symmetry axis. The direction of wave propagation is from left to right.

TABLE II. Comparison of experimental and numerical results.

Inert insert material	Distance of reliable detonation transmission, mm.		Crash distance of detonation transmission, mm	
	Left - experiments, right - calculations	Left - experiments, right - calculations	Left - experiments, right - calculations	Left - experiments, right - calculations
Without inert insert	50	45	55	50
Fluoroplastic	45	45	50	50
Copper	30	37	37	40
Silicon carbide	26	30	30	35

TABLE III. Ignition & growth parameters for cast Composition B.

Unreacted JWL	Product JWL
$A = 1479 \text{ Mbar}$	$A = 5.308 \text{ Mbar}$
$B = -0.05261 \text{ Mbar}$	$B = 0.0783 \text{ Mbar}$
$R_{1u} = 12$	$R_1 = 4.5$
$R_{2u} = 12$	$R_2 = 1.2$
$\omega_u = 0.912$	$\omega = 0.34$
$C_v = 2.487 \times 10^{-5} \text{ Mbar/K}$	$C_v = 1.0 \times 10^{-5} \text{ Mbar/K}$
$T_o = 298 \text{ }^\circ\text{K}$	$C\text{-J Energy/unit volume}$ $E_{og} = 0.081 \text{ Mbar}$
Shear Modulus = 0.035 Mbar	$C\text{-J Detonation velocity}$ $U_D = 7.576 \text{ mm}/\mu\text{s}$
Yield Strength = 0.002 Mbar	$C\text{-J Pressure}$ $P_{CJ} = 0.265 \text{ Mbar}$
$\rho_0 = 1.63 \text{ g/cm}^3$	Reaction zone width $W_{\text{rea}} = 2.5$
Von Neumann spike rel vol. $c_0 = 0.7$	Max change in reaction ratio $\Delta F_{\max} = 0.1$
$C\text{-J Energy/unit volume}$ $E_{0,u} = -0.00504 \text{ Mbar}$	
Reaction rates	
$a = 0.0367$	$x = 7.0$
$b = 0.667$	$y = 2.0$
$c = 0.667$	$z = 3.0$
$d = 0.333$	$F_{ig\max} = 0.022$
$e = 0.222$	$F_{G1\max} = 0.7$
$g = 1.0$	$F_{G2\min} = 0.0$
$I = 4.0 \times 10^6 \mu\text{s}^{-1}$	$G_1 = 140 \text{ Mbar}^{-2} \mu\text{s}^{-1}$
Maximum relative volume in tension = 1.1	$G_2 = 1000 \text{ Mbar}^{-3} \mu\text{s}^{-1}$

TABLE IV. EOS parameters for silicon carbide.

Reference density	3.10 g/cm^3
Gruneisen coefficient	1.25
Parameter C_1	$8.00 \text{ mm}/\mu\text{s}$
Parameter S_1	0.95
Strength	von Mises
Shear Modulus	1.70 Mbar
Yield Stress	0.065 Mbar
Failure	None

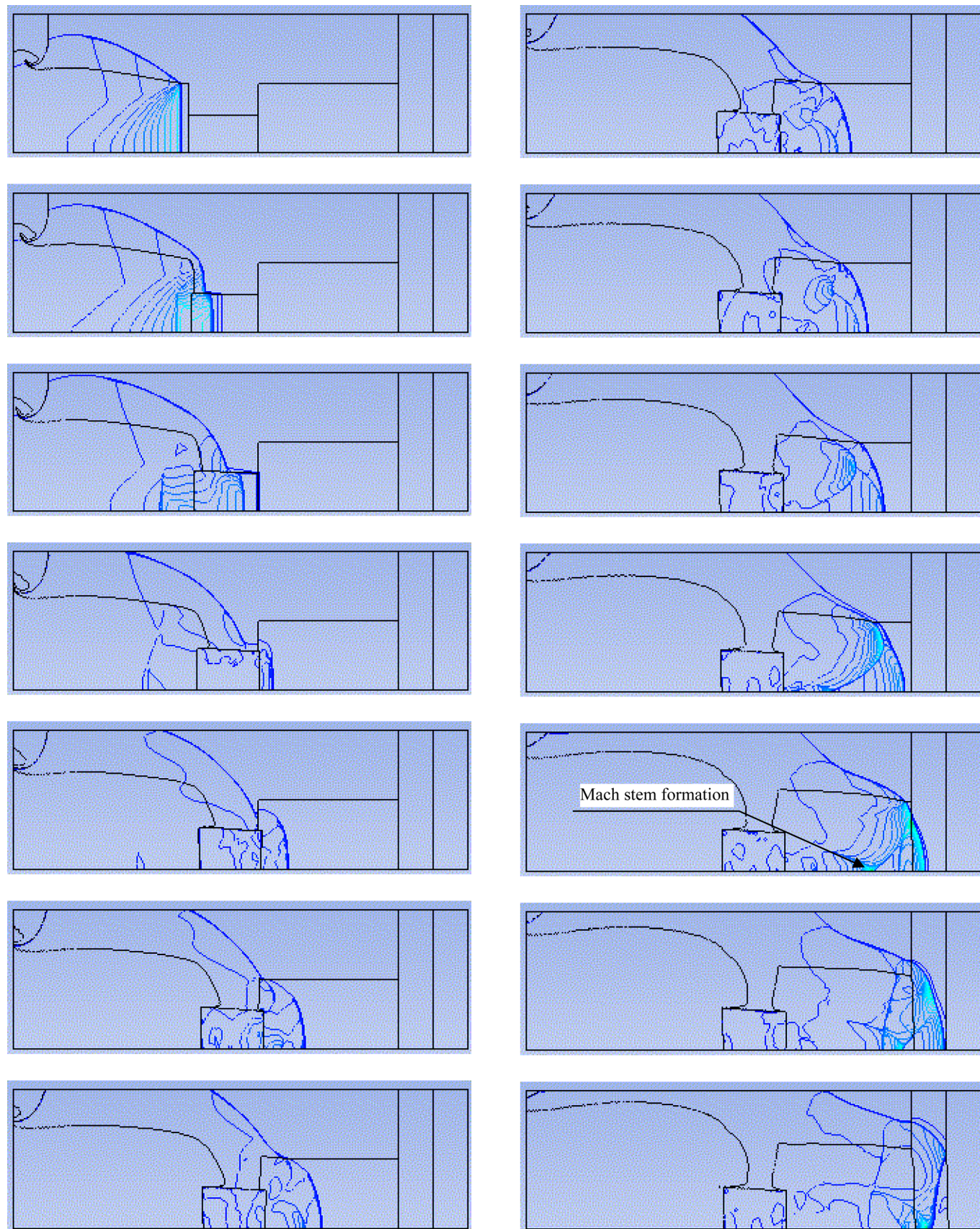


FIG. 9. (Color online) Material flow fields and pressure contours at different times with time step of $1 \mu\text{s}$. Calculated area was $x = 13 \text{ cm}$ (2600 cells), $y = 4 \text{ cm}$ (800 cells).

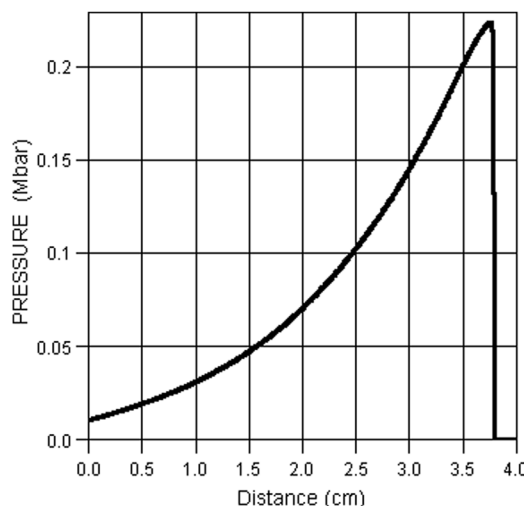


FIG. 10. Pressure profile on the symmetry axis of active HE charge at the time of $5 \mu\text{s}$ from $x_1 = 1 \text{ cm}$ to $x_2 = 5 \text{ cm}$.

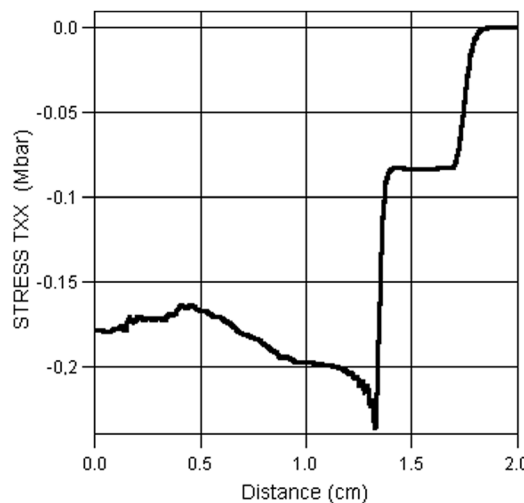


FIG. 11. Graph of the axial stress in the silicon carbide insert vs axial distance at $t = 6.75 \mu\text{s}$ from $x_1 = 5 \text{ cm}$ to $x_2 = 7 \text{ cm}$.

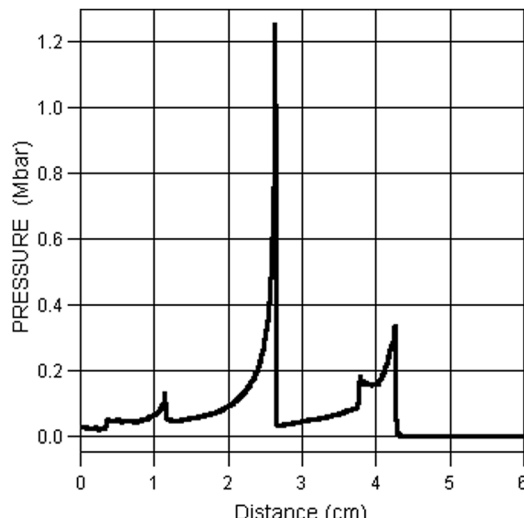


FIG. 12. Pressure graph in the passive HE charge vs axial distance at $t = 15.75 \mu\text{s}$ from $x_1 = 7 \text{ cm}$ to $x_2 = 13 \text{ cm}$.

As a result, we can observe the Mach stem formation as shown in Figs. 7 and 9. Calculated maximum pressure value in the Mach wave is 1.25 Mbar at $t = 15.75 \mu\text{s}$.

IV. CONCLUSIONS

We have observed the Mach stem formation in explosion systems that include high modulus elastic elements. It has been shown that this phenomenon is reproduced for various high explosives. The phenomenon is observed in conditions close to critical conditions of detonation transfer from an active to a passive HE charge. It is important to note that the Mach stem formation occurs in a wider range of conditions for TG-40/60 than for Composition B. This is caused, apparently, by differences in the structure of HE charges made from identical chemical compounds.

The best conditions for the phenomenon have been observed for TG-40/60 with ceramic insert heights of 16.5 mm, 18 mm, and 19.5 mm.

The physical reason of the Mach stem formation is the propagation of a convergent detonation wave into highly compressed HE. Results of metallographic analysis indirectly confirm very high pressures and temperatures for this scheme of explosion loading.

The phenomenon is reproduced in numerical simulation with maximum value of pressure in passive HE charge of 1.25 Mbar.

ACKNOWLEDGMENTS

The authors would like to thank Dr. Craig Tarver for a very useful discussion.

This work is partially supported by the Russian Foundation for Basic Research (project No. 06-08-0138).

- ¹L. A. Merzhievsky, Y. I. Fadeenko, V. A. Filimonov, and V. P. Chistyakov *Combust., Explos. Shock Waves* **10**, 233 (1976).
- ²I. A. Karpukhin, Yu. M. Balinetz, V. K. Bobolev, and B. P. Stepashkhin in *Proceedings of the Soviet Union Meeting on Detonation 22-26 August 1977* (Chernogolovka, 1977), p. 83.
- ³G. Eden and R. A. Belcher in *Proceedings of the 9th Symposium on Detonation, 28 August-1 September 1989* (Portland, OR, 1989), p. 831.
- ⁴J. Aveille, N. Carion, J. Vacellier, and J. M. Servas in *Proceedings of the 9th Symposium on Detonation 28 August-1 September 1989* (Portland, OR, 1989), p. 842.
- ⁵T. R. Neal in *Proceedings of the 6th Symposium on Detonation, 24-27 August 1976* (Coronado, CA, 1976) p. 602.
- ⁶G. J. Sharpe and J. B. Bdil *J. Eng. Math.* **54**, 273 (2006).
- ⁷I. A. Balagansky, S. V. Razorenov, and A. V. Utkin in *Proceedings of the 10th Detonation Symposium, 12-16 July 1993* (Boston, MA, 1993), p. 841.
- ⁸I. A. Balagansky, A. D. Matrosov, I. A. Stadnichenko, A. I. Glumov, and A. V. Samsonov *Mater. Sci. Forum* **566**, 207 (2008).
- ⁹I. A. Balagansky, A. D. Matrosov, I. A. Stadnichenko, A. I. Glumov, and A. V. Samsonov *Int. J. Mod. Phys. B* **22**, 1305 (2008).
- ¹⁰I. Balagansky, K. Hokamoto, P. Manikandan, A. Matrosov, I. Stadnichenko, and H. Miyoshi in *Proceedings of 16th APS Topical Conference on Shock Compression of Condensed Matter, 28 June-3 July 2009* (Nashville, TN, 2009), p. 197.
- ¹¹I. A. Balagansky, A. I. Balagansky, S. V. Razorenov, and A. V. Utkin in *Proceedings of 14th, APS Topical Conference on Shock Compression of Condensed Matter, 31 July-5 August* (Baltimore, MD, 2005), p. 835.
- ¹²B. D. Lambourn and P. W. Wright in *Proceedings of the 4th Symposium on Detonation, 12-15 October 1965* (Silver Spring MD, 1965), p. 142.
- ¹³S. D. Gardner and J. Wackerly in *Proceedings of the 4th Symposium on Detonation, 12-15 October* (Silver Spring MD, 1965), p. 154.

¹⁴AUTODYN, Explicit Software for Nonlinear Dynamics, *Explosive Initiation User Manual Century Dynamics*, 2005.

¹⁵I. A. Balagansky, K. Hokamoto, P. Manikandan, A. D. Matrosov, I. A. Stadnichenko, H. Miyoshi, I. A. Bataev, A. A. Bataev, and A. A. Stepanov in *Proceedings of the 14th International Detonation Symposium, 11-16 April 2010* (Coeur d'Alene, ID, 2010), p. 583.

¹⁶M. J. Murphy and E. L. Lee in *Proceedings of the 10th Detonation Symposium, 12-16 July 1993* (Boston, MA, 1993), p. 963.

¹⁷P. A. Urtiew, K. S. Vandersall, C. M. Tarver, F. Garcia, and J. W. Forbes in *Proceedings of the 13th Detonation Symposium, 23-28 July 2006* (Norfolk, VA, 2006), p. 929.

¹⁸C. M. Tarver, P. A. Urtiew, and W. C. Tao *J. Appl. Phys.* **78**, p. 3089 (1995).